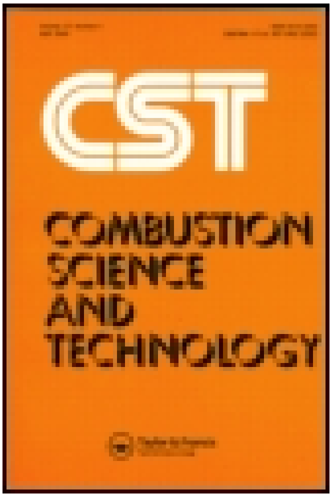

Combustion Science and Technology
Publication details, including instructions for authors and subscription information:
http://www.tandfonline.com/loi/gcst20

A 3D PHYSICAL REAL-TIME MODEL OF SURFACE FIRES ACROSS FUEL BEDS

JACQUES-HENRI BALBI [a], JEAN-LOUIS ROSSI [a], THIERRY MARCELLI [a] & PAUL-ANTOINE SANTONI [a]
[a] Université de Corse, Systèmes Physiques pour l'Environnement U.M.R.-C.N.R.S. 6134, Corte, France

Published online: 22 Oct 2007.

Combust. Sci. and Tech., 179: 2511–2537, 2007

ISSN: 0010-2202 print/1563-521X online
DOI: 10.1080/00102200701484449

A 3D Physical Real-Time Model of Surface Fires Across Fuel Beds

Jacques-Henri Balbi, Jean-Louis Rossi, Thierry Marcelli*, and Paul-Antoine Santoni
Université de Corse, Systèmes Physiques pour l'Environnement
U.M.R.-C.N.R.S. 6134, Corte, France

Abstract: This work presents a new modelling approach to the elaboration of a simple model of surface fire spread. This model runs faster than real-time and will be integrated in management tools. Until now, models used in such tools have been based on an empirical relationship. These tools may be efficient for conditions that are comparable to those of test-fires but the absence of a physical description makes them inapplicable to other situations. This paper proposes a physical 3D model of surface fire able to predict fire behaviour faster than real-time. This model is tested on experiments carried out across fuel beds under slope and wind conditions.

Keywords: Physical model; Wildland fire

INTRODUCTION

The aim of this work is to provide a model of wildland fire spread devoted to be the physical heart of a tool for fire-fighters. To proceed, that model should be able to satisfy two contradictory properties:

- P1: to be as complete as possible with regard to the equations that govern fires.
- P2: to be as simple as possible to predict fire behaviour faster than real time.

Received 17 October 2005; accepted 4 March 2007.
*Address correspondence to marcelli@univ-corse.fr

Forest fire spread modelling deals with several different approaches (Pastor et al., 2003). Following the classification of Weber (1990), one can define three kinds of modelling. The simplest models are the statistical ones, which make no attempt to involve physical mechanisms (McArthur, 1966). Empirical models (Rothermel, 1972) are based upon the conservation of energy, but they do not distinguish the mode of heat transfer. Finally, physical models differentiate the various kinds of heat transfer in order to predict fire behaviour (Albini, 1985).

Among them, multiphase modelling, which takes into account the detailed physical phenomena involved in fire spread, represents the most complete approach developed so far (Larini et al., 1997). Statistical and empirical models satisfy property P2; yet they may be very efficient for fuel and environmental conditions comparable to those of test-fires; conversely the absence of a real physical description makes them inapplicable to other situations. On the other hand, multiphase models are limited to small or medium scale line fires (length scale $<100\,\text{m}$), for which a 2D approximation in a plane defined by the direction of propagation and the vertical is assumed (Morvan and Dupuy, 2004). Among the different management tools that have been developed to date, the greater part, like FARSITE (Finney, 1998), are based upon Rothermel's model (1972), which has the disadvantage of being empirical.

In the current work we propose an alternative way for forest fire modelling capable to satisfy simultaneously both P1 and P2 requirements thanks to several simplifying assumptions. The resulting model leads to a quasi-analytic solution for predicting the fire spread rate. Most of the experimental results, provided at laboratory scale by different authors (Dupuy, 1995; Guijarro, 1997; Mendes-Lopes et al., 2003; Viegas, 2004) for fire spread under slope or/and wind conditions, are depicted by the model. But, it has also been tested for field fires (Martins-Fernandes, 2001). This model can be classified as physical and gives a 3D flame front. The main heat transfer mechanisms are differentiated in its formulation, and its parameters, which are fuel dependant, are obtained from the fire dynamic. It can be viewed as a set of four simplified sub-models for modelling: the flow, the flame, the radiation and the fuel preheating.

MODELLING APPROACH

Simplified Flow and Flame Tilt Angle

The major part of the calculation time in problems of combustion is due to the equations governing the flow. To reach our aim, which is to elaborate a simulator working faster than real time, the gas phase equations have to be drastically simplified. To proceed, we will assume that the main effect of the flow that must be taken into account is the tilting of the flames under wind or/and slope conditions. Indeed, we can distinguish two regimes for spreading fires. The first one occurs under zero wind and no slope. Forest fires spread slowly with rather a constant velocity for a given fuel. The other one is encountered under slope and/or wind conditions for which fires accelerate strongly due to tilted flames (Dupuy, 1995; Mendes-Lopes et al., 2003; Viegas, 2004). Flame tilt angle, which is responsible of forest fire dynamics, is the variable calculated here instead of the flow equations. In order to evaluate it, we assume that:

Under wind and no slope, the flame tilt angle γ equals to β_w, which results from the competition between buoyancy and wind. We showed (Morandini et al., 2001) that β_w is given by

$$\tan \beta_w = \frac{v_w}{u_{fl}} \tag{1}$$

where v_w and u_{fl} represent the free stream wind speed and the upward gas flow velocity in still air, both at mid-flame, respectively. Whether the wind velocity $\vec{v}_w$ is not in the direction of the normal of the fire front, $\vec{n}$, the flame tilt angle along $\vec{n}$ is given by Eq. (1) where $v_w = \vec{v}_w \cdot \vec{n}$.

- Under up-slope condition, the flame tilt angle, γ (see Figure 1a) due to gas velocity induced by in draft, v_s, and slope angle α_0 is given by the following relationships

$$\gamma = \alpha + \beta_s \tag{2}$$

$$\tan \beta_s = \frac{v_s}{u_{fl}} \tag{3}$$

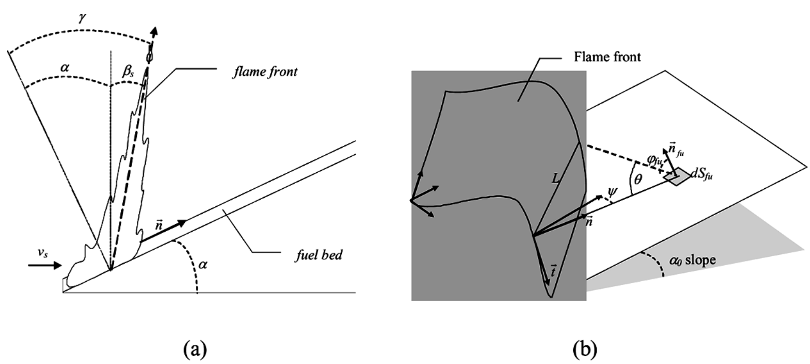

Figure 1. (a). Flame tilt angle under up-slope condition. (b). Location of Ψ.

$$\sin\alpha = \frac{\sin\alpha_0 \cos\psi}{(\sin^2\alpha_0 \cos^2\psi + \cos^2\alpha_0)^{1/2}} \tag{4}$$

where α represents the local slope angle (see Figure 1a), ψ is the angle located between the normal of the fire front and the direction of the greatest slope α_0 (see Figure 1b).

- For combined wind and slope conditions, we assume that gas velocity induced by in draft is neglected in regard with free wind velocity. Hence:

$$\gamma = \alpha + \beta_w \tag{5}$$

where β_w is given by Eq. (1).

Simplified Flame Sub-Model

At this point, we have to calculate u_{fl} and v_s at the flame level. However, to reach our aim, which is to elaborate a simulator working more fastly than real-time, it is necessary to make some simplifying assumptions in order to generate a simple model of flame. Let assume that the flame is made of two main regions (see Figure 2). The first one, called "the flame base," is attached to the fuel bed. Let D its depth and h its height. The second one, called "the flame body" is the classical fire plume. Let l its depth and H its height.

Flame Height. The flame height is calculated from the following empirical correlation established for static fires by McCaffrey (1979), and recently by Sun et al. (2003) for vegetation fires:

$$H = H^* Q^{2/5} = H^*(\Delta h_{fu}\sigma_{fu}c)^{2/5} \tag{6}$$

where H represents the flame height (see Figure 2), Q is the rate of heat release per unit length of fire front and H^* a parameter to fit. We assume that Eq. (6), which was elaborated for square burners, remains valid for a spreading fire line. In the calculation of Q, Δh_{fu} represents the heat of combustion of the vegetative fuel, σ_{fu} its surface mass and c is the rate of fire spread.

State Equation. We consider the gas state equation for the quasi-isobaric diffusion flame:

$$\rho_g T_g = \rho_a T_a \tag{7}$$

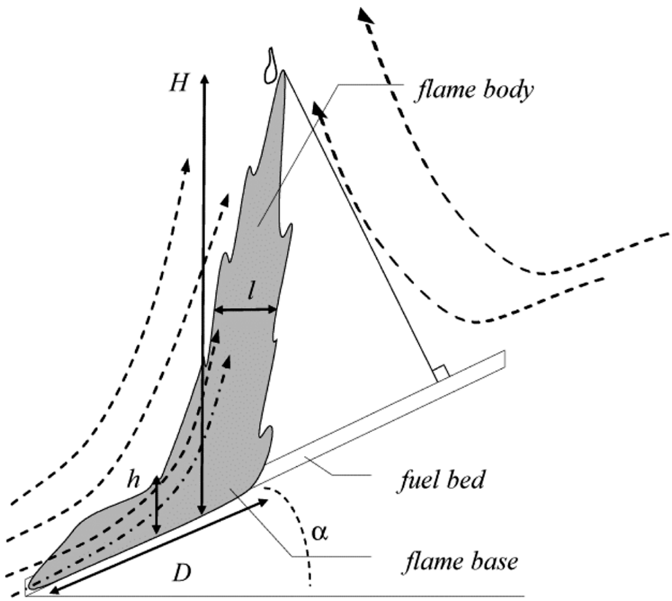

Figure 2. Definition of the geometrical characteristics used for the flame.

Vertical Momentum Equation. By neglecting the shear stresses in the gas phase and by considering the buoyancy effects as the fundamental mechanism involved in the momentum equation, the vertical component of the gas velocity is given by:

$$\rho_g \frac{du}{dt} = (\rho_a - \rho_g)g.$$

Or $u^2 = 2g^* z$ with $g^* = g\left(\frac{\rho_a}{\rho_g} - 1\right)$ and $z = \frac{H}{2} = \frac{H^*}{2} Q^{2/5}$.

After integration along the flame, we obtain the gas velocity at mid-flame, u_{fl}:

$$u_{fl} = Q^{1/5} \sqrt{\left(\frac{T_{fl}}{T_a} - 1\right) g H^*} \tag{8}$$

Mass Balance. A simplified mass balance is proposed for the whole flame structure, based on the geometrical flame characteristics displayed in Figure 2. Under slope or wind condition, we assume that the rate of air entrainment, respectively downward and downwind, is negligible in the mass balance. Hence, the continuity equation per unit length of the fire line is given by

$$\rho_g u_{fl} l = \rho_{ga} h v_u + D\dot{\sigma}_{fu}$$

The term on the left hand side of that relationship represents the rate of mass loss from flame body. The first term on the right hand side is the rate of air entrainment upward or upwind in the flame. The last term is the rate of mass increase due to the thermal degradation of the vegetation.

Stoichiometric Ratio. If we further assume that the rate of air entrainment upward in the flame is proportional to the rate of mass incoming from thermal degradation, υ being the stoichiometric coefficient:

$$\rho_a h v_u = \upsilon D\dot{\sigma}_{fu} \tag{9}$$

the simplified mass balance can be written

$$\rho_g u_{fl} l = (\upsilon + 1) D\dot{\sigma}_{fu} \tag{10}$$

Thermal Balance. The thermal balance is written with the same assumptions as those for the continuity equation.

$$\rho_g c_{pg} u_{fl} l T_{fl} - (\rho_{ga} c_{pg,a} h v_u T_a + D\dot{\sigma}_{fu} c_{pg,fu} T_{g,fu}) = (1 - \chi) Q$$

where χ represents the fraction of the energy liberated per unit time by the reaction and due to radiation (Markstein, 1977). If we further assume that the specific heat is constant and equal everywhere in the flame (C_{pg}), in ambient ($C_{pg,a}$) and in the fuel gases ($C_{pg,fu}$) and that the fuel gases are emitted near ambient temperature ($T_{g,fu} = T_a$), we obtain

$$T_{fl} = T_a + \frac{(1-\chi)Q}{(\upsilon + 1) D\dot{\sigma}_{fu} c_{pg}} = T_a + \frac{(1-\chi)\Delta h_{fu}}{(\upsilon + 1) c_{pg}} \tag{11}$$

Simplified Radiation Sub-Model

When fire front spreads, the radiant heat flux impinging on the unburned fuel ahead of the flame is the sum of two contributions. The first one, R_b, is due to the flame base and the embers. The second one, R_{fl}, comes from the flame body. By assuming that emissivity of the flame base is equal to unity (due to the presence of embers) R_b is given by

$$R_b = \sigma T_{fl}^4 d(\delta - x) \tag{12}$$

where T_{fl} is the flame temperature, $\delta = 4/(\alpha_{fu} \xi_{fu})$ is the mean penetration distance of radiation (de Mestre et al., 1989) within the fuel bed, x is the coordinate in space normal to the fire front and d represents the fuel depth. When fire spreads on an inclined surface or for wind driven fire, flames are brought closer to the unburned fuel and the resulting radiant heat flux impinging on the unburned fuel is increased, increasing the spread rate. This effect is mainly due to R_{fl}. Starting from a formulation used to evaluate the radiation from radiant surfaces, we propose an original simplification to calculate R_{fl}, suitable to our objective i.e., a robust model to be used in a fire management tool. The flame is commonly modelled as a radiant surface (Weber, 1989) with a given height, constant temperature T_{fl} and emissivity ε_{fl}. The amount of radiant energy impinging the top of the litter is determined by means of the Stefan–Boltzmann law. This law allows to determine the part of radiation emitted from an element of the flame front of area dS_{fl} which impinges on unburned fuel element dS_{fu}. This amount of energy is attenuated according to an inverse square law of the distance r between the two areas and also depends on the cosine of angles φ_{fl} and φ_{fu} defined between the ray and the normal of dS_{fl} and dS_{fu}, respectively. The rate at which the radiant energy from the surface of the flame front S_{fl} is absorbed by a fuel element is given by

$$R_{fl} = \varepsilon_{fl}\sigma T_{fl}^4 \int_{S_{fl}} \frac{\cos\varphi_{fl}\cos\varphi_{fu}}{\pi r^2} dS_{fl} dS_{fu} \tag{13a}$$

In order to calculate R_{fl} more fastly than in real-time, we will derive an analytical expression from Eq. (13a). Provided that the fire front can be viewed as a flame panel of the same height H and of infinite width from a surface fuel element, we obtain

$$R_{fl} = \varepsilon_{fl}\sigma \frac{T_{fl}^4}{2}(1 - \cos\theta) \tag{13b}$$

where θ is displayed in Figure 1b. It represents the angle located between the direction given by the base of the flame panel and the element of surface fuel on the one hand and the direction given by the height of the flame panel and the element of surface fuel on the other hand.

Preheating Sub-Model

In this last sub-model, we assume that radiation is the prevailing heat transfer involved in fire spread. The thermal balance for the unburned fuel ahead of the fire front is given by

$$\sigma_{fu} c_{pfu} \frac{dT_{fu}}{dt} = R_b + R_{fl} - \Delta h_w \frac{d\sigma_w}{dt} \tag{14}$$

where σ_w represents the surface mass of water in fuel (kg/m^2).

Quasi-Analytic Solution

As previously mentioned, there exist two regimes for forest fires. The first one occurs under zero wind and no slope. Forest fires spread slowly with rather a constant velocity for a given fuel. The other one is encountered under slope and/or wind conditions for which fires accelerate strongly due to tilted flames (Dupuy, 1995; Mendes-Lopes et al., 2003; Viegas, 2004). We have modelled those regimes as follows:

Relationship for the Rate of Spread under Low Speed Regimes. In those cases, fires are mainly driven by the radiant action of the flame base since the flame body is not tilted toward the unburned fuel. Eq. (14), with R_{fl} neglected leads to

$$\sigma_{fu} c_{pfu} \frac{dT_{fu}}{dt} = R_b - \Delta h_w \frac{d\sigma_w}{dt}$$

Since $dx = c_l \, dt$, this relationship becomes

$$\sigma_{fu} c_{pfu} c_l \frac{dT_{fu}}{dx} = \sigma T_{fl}^4 d(\delta - x) - \Delta h_w c_l \frac{d\sigma_w}{dx}$$

By integrating this last result from 0 to δ, ahead of the fire front and, taking c_l constant in this space interval we obtain

$$\sigma_{fu} c_{pfu} c_l (T_{ig} - T_a) = \frac{1}{2} \sigma T_{fl}^4 d\delta^2 - \Delta h_w c_l \eta \sigma_{fu}$$

Where η represents the moisture content defined by $\eta = \sigma_w / \sigma_{fu}$. Finally we have

$$c_l = \frac{\sigma T_{fl}^4 d\delta^2}{2\sigma_{fu}(c_{pfu}(T_{ig} - T_a) + \Delta h_w \eta)} \tag{15}$$

Relationship for the Rate of Spread under High Speed Regimes. In those cases, we suppose that the effects of the radiant heat flux are negligible ahead of the projection of the flame height upon the fuel bed, given by $H \sin\gamma / \cos\beta$. By assuming that the rate of spread, c_h is constant over the space interval [0, $H \sin\gamma$], Eq. (14) integrated on that time step leads to

$$\sigma_{fu} c_{pfu} c_h (T_{ig} - T_a) = \frac{1}{2} \sigma T_{fl}^4 d\delta^2 + \frac{\varepsilon_{fl} \sigma T_{fl}^4 H}{2} (1 + \sin\gamma - \cos\gamma) - \Delta h_w c_h \eta \sigma_{fu}$$

Thus,

$$c_h = c_l + \frac{\varepsilon_{fl} \sigma T_{fl}^4 H}{2\sigma_{fu}(C_{pfu}(T_{ig} - T_a) + \Delta h_w \eta)} (1 + \sin\gamma - \cos\gamma)$$

Furthermore, since c_l is negligible with regard to c_h (Dupuy, 1995; Mendes-Lopes et al., 2003; Viegas, 2004;), we have the approximation

$$c_h \approx \frac{\varepsilon_{fl}\sigma T_{fl}^4 H}{2\sigma_{fu}(C_{pfu}(T_{ig} - T_a) + \Delta h_w \eta)}(1 + \sin\gamma - \cos\gamma) \tag{16}$$

Simplified Model of Fire Spread under High-Speed Regimes. The rate of radiant heat transfer from the flame surface is given by

$$\varepsilon_{fl}\sigma T_{fl}^4 = \chi Q/H$$

In order to reach the final form of the model we do the following hypothesis: the fraction of radiation χ decreases with flame width, according to $\chi = 0.3(\frac{c_h}{c_l})^{-1/q}$ where q is a parameter which must be fitted.

The model can be rewritten under the three previously defined high regimes, i.e. slope alone, and wind combined with slope or alone:

$$\begin{cases} \dfrac{c_h}{c_l} = A(1 + \sin\gamma - \cos\gamma)^q \\ \gamma = \alpha + \beta_s \\ \tan\beta_s = b_s c_h^{3/5} \\ \text{with } b_s = \dfrac{\tau}{0.08(\Delta h_{fu}\sigma_{fu})^{2/5}} \\ \text{under slope condition(see Eq. (22) in Appendix for calculation of } b_s) \end{cases} \tag{17}$$

$$\begin{cases} \dfrac{c_h}{c_l} = A(1 + \sin\gamma - \cos\gamma)^q \\ \gamma = \alpha + \beta_w \\ \tan\beta_w = b_w v_w c_h^{-1/5} \\ \text{with } b_w = \dfrac{1}{0.2\sqrt{\left(\frac{T_{fl}}{T_a} - 1\right)g}(\Delta h_{fu}\sigma_{fu})^{1/5}} \\ \text{under wind and both wind and slope (see Eq. (23) in Appendix,} \\ \text{calculation of } \mathrm{b_w}) \end{cases} \tag{18}$$

$$\text{with } A = \left(\frac{0.15\Delta h_{fu}}{C_{pfu}(T_{ig} - T_a) + \Delta h_w \eta}\right)^q \tag{19}$$

NUMERICAL METHOD

Here we describe the numerical method used to determine the model parameters of the two nonlinear equations (see Eqs. (17) or (18)) and we also describe the method applied to calculate and visualize the spread of the fire front shape on a three-dimensional domain (see Figure 3).

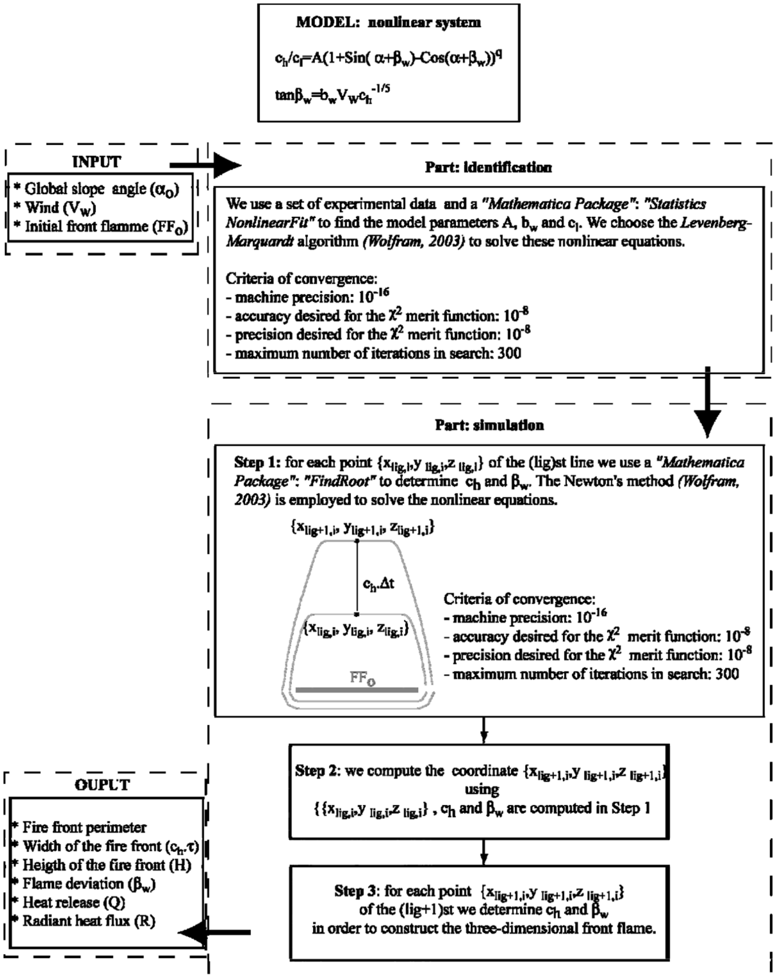

Figure 3. Iteration process.

Determination of the Parameters: Identification

To find the model parameters A, b_w and b_s, we use a *Mathematica Package (Wolfram, 2003): "Statistics NonlinearFit."* This Package provides a numerical solution to the mathematical problem of minimizing a sum of squares of several, nonlinear functions that depend on a common set of parameters. The Levenberg–Marquardt algorithm (LMA)is used to solve these nonlinear equations (see Eqs. (17) or (18)). The LMA interpolates between the Gauss–Newton algorithm (GNA) and the method of gradient descent. We choose the LMA because it is more robust than the GNA. This means that in many cases it finds a solution even if it starts very far away from the final solution.

Determination of the 3D Shape of Fire Front: Simulation

To visualize the fire front shape, we begin at time $t = 0$ with the given ignition position line (see Figure 3). This line consists of n points. The position of a point i is given by the coordinates $\{x_{0,i},\ y_{0,i},\ z_{0,i}\}$. The time is incremented by Δt in each step of an outer loop until the final time t_{end} is reached. At time step lig, the value of c_h is calculated (Eqs. (17) or (18)) for each point and those permit to determine the $(lig + 1)$ line position (see Figure 3). To visualize the fire front shape on a three-dimensional domain, we calculate not only c_h but also g (see Figure 4). So, in every time step and for each line point, this method requires the solution of a nonlinear system. In short, the basis for the computation of the spread of the fire front shape lies in calculating the position of the fire front at the time $t_{lig+1} = t_{lig} + \Delta t$ given it position at time t_{lig}. This occurs in four steps:

Step 1: For each point $\{x_{lig,i},\ y_{lig,i},\ z_{lig,i}\}$ *of the (lig)st* line, solve the nonlinear system (Eqs. (17) or (18)) in order to determinate c_h and γ.

Step 2: Compute the coordinate $\{x_{lig+1,i},\ y_{lig+1,i},\ z_{lig+1,i}\}$ using $\{x_{lig,i},\ y_{lig,1,i},\ z_{li1,i}\}$, c_h and γ computed in Step 1.

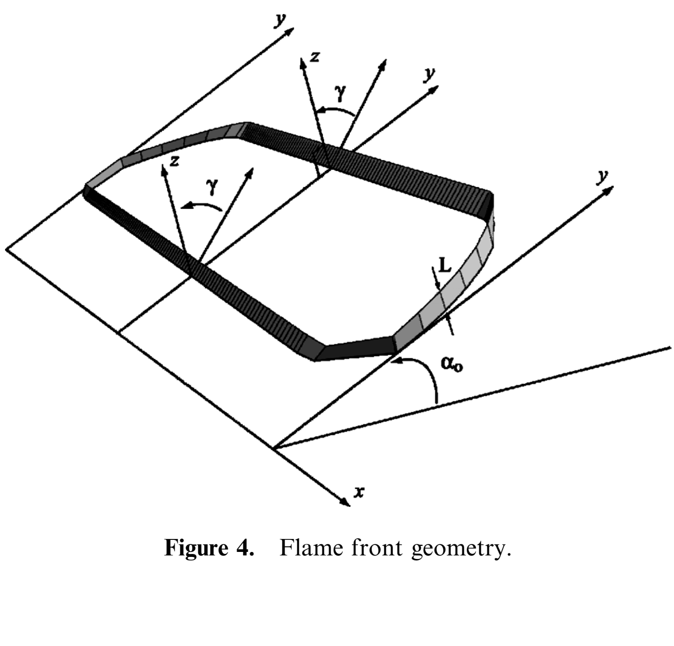

Figure 4. Flame front geometry.

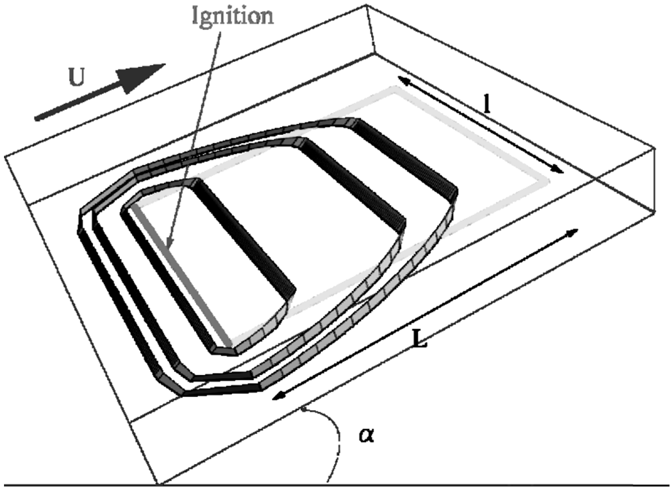

Figure 5. 3D fire front evolution.

Step 3: For each point $\{x_{lig+1,i}, y_{lig+1,i}, z_{lig+1,i}\}$ *of the (lig+1)st* determine c_h and γ in order to construct the three-dimensional front flame.
Step 4: Use *Mathematica's* own graphic capabilities to represent the fire front shape on a three-dimensional domain (see Figure 5).

We can note that this algorithm does not require covering the plot with a grid. Consequently, computational time is lower than real-time. For example, for a simulation time of 2000 s and a line consisting of 200 points, the computational time is only 33.3 s.

MODEL VALIDATION: RATE OF SPREAD

After the comparison with some existing models, it is important to test the model with experimental data. Three sets of experimental data obtained from fires spreading across pine needles are considered (Guijarro et al., 1997; Mendes-Lopes et al., 2003; Viegas, 2004) at laboratory scale, and a set of experimental burns (Martins-Fernandes, 2001) at field scale fires. To test the two variants of our simplified model, we split those data sets into two categories: with and without wind.

Laboratory Fires

Laboratory Experiment 1: Wind (Mendes-Lopes et al., 2003)—Experimental Procedures. The first set of experimental data (Mendes-Lopes et al., 2003) concerns experiments carried out at the Instituto Superior Tecnico (I.S.T.) of Lisboa (Portugal) under both combined wind and upslope conditions. The wind speed values covered a range between 1 to 3 m/s (step 1 m/s) and the movable tray could be set at angles from 5 up to 15°(step 5°) with upslope orientation (see Figure 6). The fuel bed made up of needles of *Pinus pinaster* occupies 0.70 m wide and 2 m long with a load of 0.5 kg/m^2 on dry basis and a fuel moisture content of 10% (±1%).

Results and Discussion. Figure 7 shows the predicted rate of spread versus the observed ones. The model parameters A, b_w and q were fitted on the whole data set, i.e., the wind ranged from 1 to 3 m/s and the slope ranged from 0 to 15°. The predicted rates of spread are close to the observed ones. The model represents the rate of spread growth according to slope and wind.

In order to validate the parameters fitting method and the model, we fitted the three parameters on a data subset. We only used wind values for a fixed slope (10°), and then we proceeded to verification for the whole data set. Once again, the model represents well the evolution of the rate of spread versus slope and wind. The mean relative error done on the parameters fitting (see Figure 7a) is 6.54% with a correlation coefficient of 0.9836. This error is 8.81% for a fitting on an experimental data subset with a correlation coefficient of 0.9832.

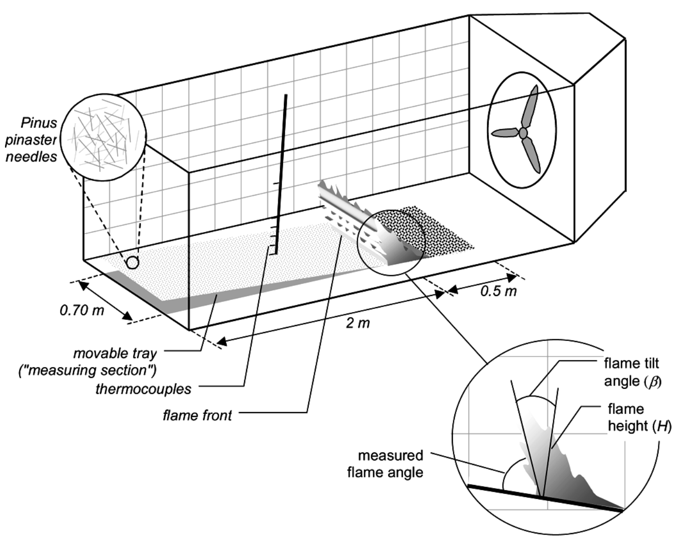

Figure 6. Sketch of the wind tunnel.

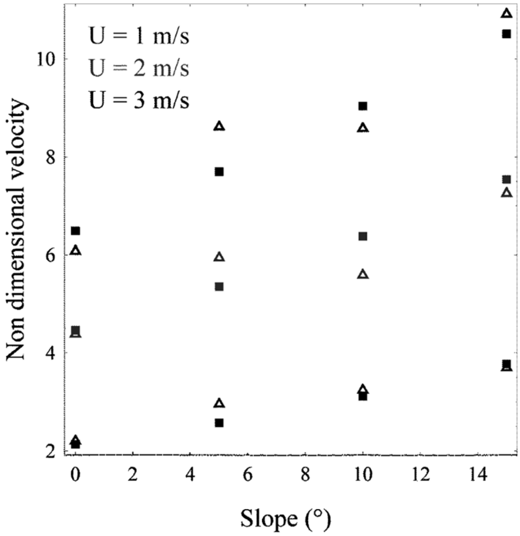

(a) △experimental, ■predicted

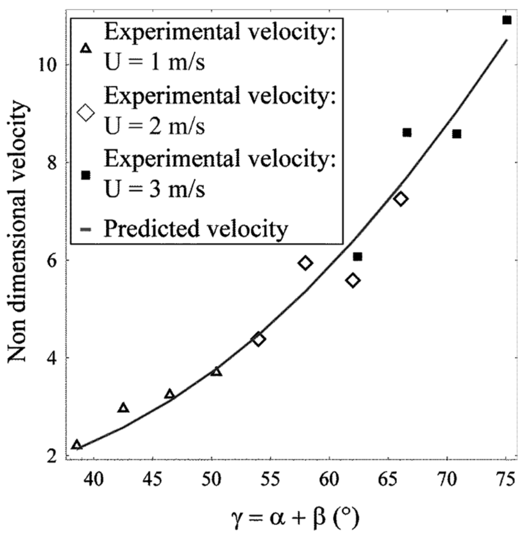

(b)

Figure 7. Experiment 1 (Mendes-Lopes et al., 2003): Predicted and observed rates of spread. Fitting on the whole set of experimental data. (a) Non-dimensional velocity versus slope, (b) non-dimensional velocity versus flame tilt angle. ($A = 1.239$, $b = 0.927$, $q = 3$).

So, whatever the data subset used to fit the three parameters (A, b_w, q), we obtain the same values with small deviations. We use the remaining data to test the model. The most important parameter is the power q: it is always found close to 3, and now we fix $q = 3$, making it a universal parameter. Thus for the following experiments, two parameters to fit are remaining. Figure 8 which represents the rate of spread versus γ (given by the model), shows the suitability of this 3-power function.

Laboratory Experiment 2: Wind (Guijarro et al., 1997)

Experimental Procedures. Tests were conducted in the combustion tunnel of INIA. The said tunnel consists of a heat area with the following dimensions: 8.5 m long and a transversal section of $2\,m \times 3\,m$; on the ground there are eight independent small wagons 1 m long $\times$ 0.8 m wide and 0.25 m high, filled with gravel and covered with a sand layer, so that they form a surface of $8\,m \times 0.8\,m$ on which the fuel, bed of needles of *Pinus pinaster*, is arranged. The tunnel is equipped with a fan intended to create an air flow, feigning the action of wind the heat area; the fan is controlled by an electronic system which enables to obtain wind speed values between 1 and 7 m/s in the central area of the heat area.

Two fuel load values (0.5 and 1 kg/m^2) and four wind speed values (0, 1, 2 and 3 m/s) were selected. For each load and wind speed, three replications were made. Tests were carried out with low fuel moisture content, around 10%.

Results and Discussion. As in the previous experiment, we fix $q = 3$, and fit the parameters A and b_w. According to our model, A does not vary with the surface mass σ when b_w varies like $\sigma^{-1/5}$. The values for the parameters are (see Figure 8):

- $\sigma = 0.5\,kg/m^2$: $A = 1.61$ and $b_w = 0.87$
- $\sigma = 1\,kg/m^2$: $A = 1.61$ and $b_w = 0.82$

We can observe that the parameter b_w varies as predicted by the model. We can compare those results to those obtained for experiment #1 (Mendes-Lopes et al., 2003), which used *Pinus pinaster* needles with $\sigma = 0.5\,kg/m^2$, and the same fuel moisture content. Parameters A and b_w are close to those obtained in experiment #1; the small deviations are due to the experimental conditions, particularly dimensions, which are not the same in the two experiments.

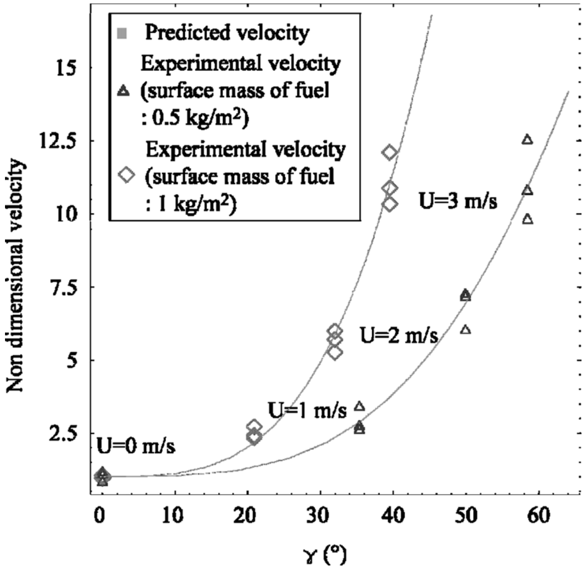

Figure 8. Experiment 2 (Guijarro et al., 1997): Non-dimensional velocity versus flame tilt angle. ($\sigma = 0.5\,\mathrm{kg/m^2}$: $\mathrm{A} = 1.61$, $\mathrm{b_w} = 0.87$, $\mathrm{q} = 3$; $\sigma = 1\,\mathrm{kg/m^2}$: $\mathrm{A} = 1.61$, $\mathrm{b_w} = 0.82$, $\mathrm{q} = 3$).

Laboratory Experiment 3: (Viegas, 2004)

Experimental Procedures. This set of experimental data (Viegas, 2004) concerns experiments performed at the University of Coïmbra (Portugal) under wind or upslope conditions. The wind speed values covered the range between 1.5 to 4.5 m/s (step 1.5 m/s). The bench of combustion could be set at angles from 0 up to 40°(step 10°). The fuel bed made up of needles of *Pinus pinaster* is 2 m wide and 6 m long, with a load of 1 kg/m^2 on dry basis and fuel moisture content between 8 and 13%.

Results and Discussion. Here, we have to explain the two variants of the model: under wind condition and under slope condition without wind. In both cases, and in order to have a universal parameter q (translating the surface volume ratio of the flame) we fit the parameters fixing, *a priori*, $q = 3$, as in the previous cases. So, we fit the parameter A (which depends on the fuel moisture content) and the parameters b_s and b_w. We obtain the results shown on Figures 9 and 10. We obtain:

- wind condition $q = 3$, $A = 1.49$, $b_w = 0.76$
- slope condition $q = 3$, $A = 1.49$, $b_s = 0.13$

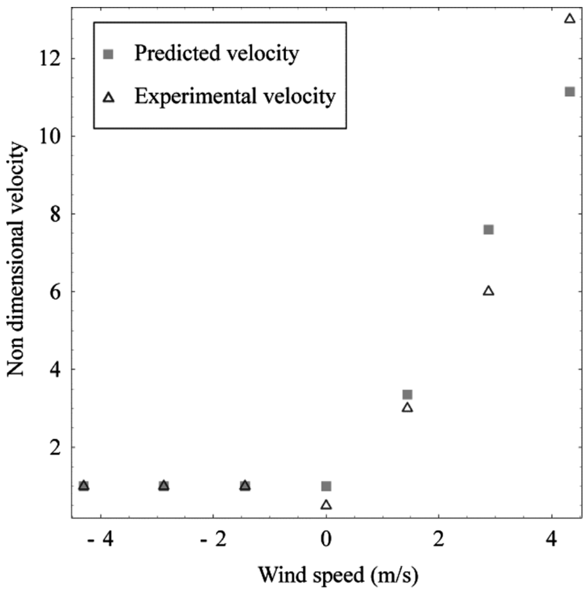

Figure 9. Experiment 3 (Viegas, 2004): Non-dimensional velocity versus wind speed. (A = 1.49, b = 0.76, q = 3).

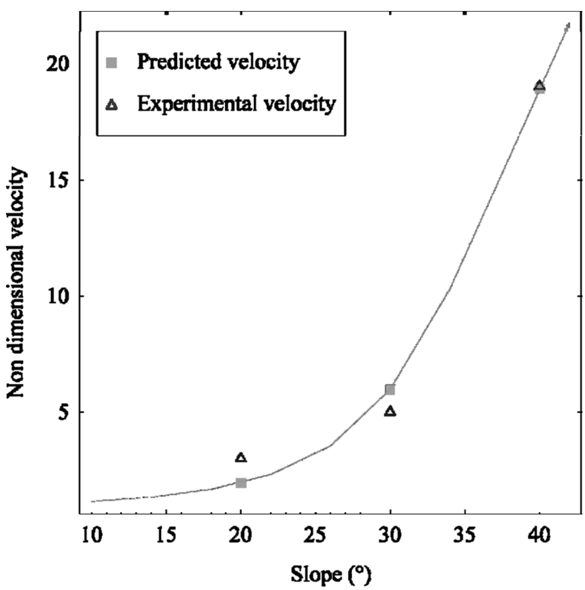

Figure 10. Experiment 3 (Viegas, 2004): Non-dimensional velocity versus slope. (A = 1.49, b = 0.13, q = 3).

The parameter A is the same in both cases in accordance with the model since it only depends on the nature of vegetation, and especially on the fuel moisture content, which are the same in both cases. In the opposite, parameters b_w and b_s are different, as predicted by the model. It is important to emphasize that this experience is the only one which has high values of slope (40°) and wind (4.3 m/s). Most literature models underestimate these values: our model gives good results even in those extreme conditions.

Wildland Fires (Martins Fernandes, 2001)

The author (Martins Fernandes, 2001) analyzed results from 29 field-scale fires for different vegetations in Portugal: no slope, wind speed ranging from 0 to 25 km/h, line ignition ranging from 10 to 100 m. With a statistical study, he establishes that the principal variables for rate of spread evolution are: the wind, and also the fuel moisture content and the height of the vegetation. He derives the following statistical model:

$$c_h = c_0 \exp(-0.067\eta) \exp(0.092U) d^{0,932} \tag{20}$$

We compare it with our physical model:

$$\left.\begin{array}{l} c_h \approx c_l A(1+\sin\beta-\cos\beta)^3 \\ \tan\beta = b_w U c_h^{-1/5} \\ (15) \Rightarrow c_l = c_{l0}(1+a\eta)^{-1} d, \\ (19) \Rightarrow A = A_0(1+a\eta)^{-3} \end{array}\right\} \Rightarrow c \approx c_{l0} A_0 (1+a\eta)^{-4}(1+\sin\beta-\cos\beta)^3 d \tag{21}$$

We fit parameters $c_{10}A_0$, a, b_w thanks to statistical model values and we obtain: $c_{10}A_0 = 1.0295$, $a = 0.6162$, $b_w = 0.7515$.

We have to emphasize the importance of this result. Martins-Fernandes (2001) has analysed 29 instrumented field-scale fires with a line ignition about 100 m long. This database is very sound. The author has deducted a statistical model which gives the rate of spread in terms of three quantities: wind, fuel moisture content and vegetation height. This model conveys decently the set of field-scale fires. In our model, the three quantities appear explicitly, and its parameters are identified ($c_{10}A_0$, a, b_w). An agreement between the models (see Figure 11) is almost perfect.

Thus, our model is validated at field scale. So, it is usable at this scale as it is at the laboratory scale, with the same parameter $q = 3$; parameters A and b_w depend on the considered vegetation (nature, surface mass, moisture content).

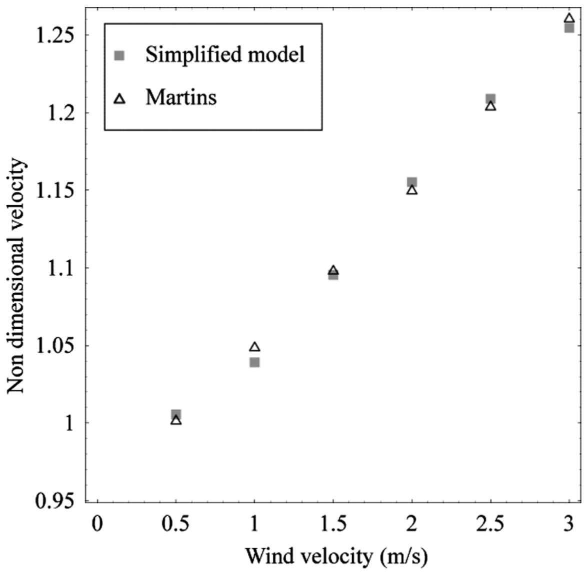

Figure 11. Wildland fires (Martins Fernandes, 2001): Non-dimensional velocity versus wind velocity.

COMPARISON TO OTHER LITERATURE MODELS

To show the contribution of our approach, a confrontation with some models of the literature (Anderson and Rothermel, 1965; Catchpole et al., 1998; Porterie et al.; 2000; Morandini et al., 2005) is presented in this section. Following Weber (1990), these models can be classified as follows:

- The models of Anderson and Rothermel (1965) and that of Catchpole et al. (1998) are semi-empirical since they involve no distinctions between the different modes of heat transfer (conduction, convection and radiation).
- The model of Morandini et al. (2005) as well as the approach proposed in the present paper are physical models. They account each mechanism of heat transfer and production individually. The model of Morandini et al. (2005) incorporates a reaction-diffusion equation for the thermal balance and a simplified one-dimensional formulation represents the flow in the fuel layer. A radiant panel assumption is performed to model the flame. It allows calculating the radiant heat transfer impinging on the top of the fuel bed ahead of the fire front. However, the flame length is assumed to be known *a priori*, which is a limitation of this model.

- The approach of Porterie et al. (2000) is also a physical model which can be view as an extension of Grishin's (1997) two-phase formulation. It considers a gas phase flowing through a bed, which is viewed as an agglomeration of organic, randomly-oriented fuel elements. A detailed description of the heat and mass transfer mechanisms, combustion and turbulence is done. Due to the important time of calculation, this approach is limited up to now to line fires for which a 2D approximation in a plane defined by the direction of propagation and the vertical is done.

The predicted and experimental (Mendes-Lopes et al., 1998) rates of spread are provided in Figure 12 for horizontal spread and wind velocity ranging from 0 to 3 m/s. The predictions are compared to the experimental data when the steady state is reached. They show that the fire rate of spread increases with increasing wind velocity. The fire behaviour predicted by the present model is particularly well represented in comparison to other modelling approaches. The model of Anderson and Rothermel (1965) fails to describe the experimental rate of spread for the highest wind velocity although the dependence of spread on wind speed is given. The purpose of semi-empirical models is mainly restricted to the prediction of the rate of spread. They do

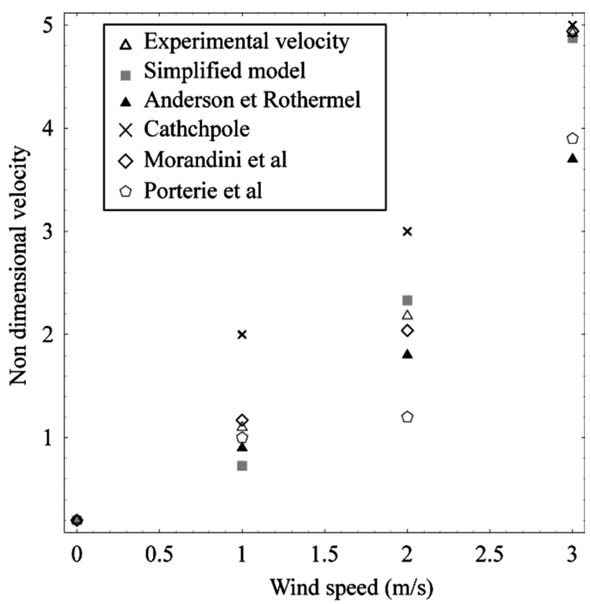

Figure 12. Comparison between some predicted models and experimental data (Mendes-Lopes et al., 1998).

not use any physical modelling to describe the heat transfer from the burning zone to the unburnt fuel.

These models may be very efficient for fuel and environmental conditions comparable to those of the test-fires used to tune them but the absence of a real physical description make them inapplicable in other situations. The model of Catchpole et al. (1998) overestimates the experimental rate of spreads. Furthermore it shows an approximate linear dependence of rate of spread on wind speed. It does not represent the trend of the increase in spread rate with increasing wind velocity. The model of Porterie et al. (2000) is also unable to follow the experimental tendency. Although the structure of this model is very sound, conversely it possesses a great set of sub models (heat transfer in porous medium, gaseous kinetic for combustion, thermal degradation of fuels, drag forces) used to close it. Those sub-models need improvement to allow better predictions. The approach of Morandini et al. (2005) agrees with experiment. Nevertheless, it should be recalled that the flame height is an input of that model that limit its use. With regard to the two last models depicted here, another disadvantage lies in their time of calculation as will been shown hereafter.

Figure 13 presents a qualitative comparison between computational time of different kinds of models. For a few minutes'' fire spread at laboratory scale, the results are as follows:

- For detailed models (bi-dimensional xz), which require solving a complex set of partial differential equations, computational time is about 1 day;
- For reduced models (bi-dimensional xy), which use one partial differential equation (energy equation), computational time is lower than the one of detailed models, and it is about a few hours;

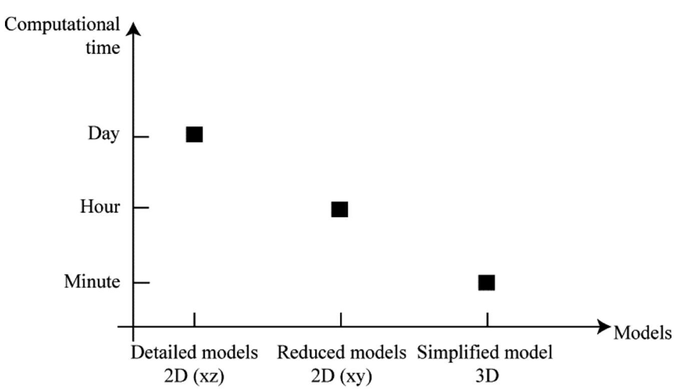

Figure 13. Computational time of different models.

- On the other hand, the present model (simplified model) has computational time of about one minute, that is to say, lower than real-time. This performance level is due to the model structure (algebraic model and quasi-analytic solution) which does not require temporal and spatial discretization of the study domain and provides results in three dimensions.

CONCLUSION

We have now a model which satisfies both properties:

- P1. It is a physical model, i.e., a model which conveys phenomena through physical laws (except flame height when an empirical relation is used); even if these laws are simplified, most of the phenomena are represented.
- P2. Computational time is about 20 times lower than real time: this is the only physical model able to do that.

The model is constituted by algebraic relations which provide the rate of spread with the knowledge of external wind (intensity and direction), the slope and the vegetation. Furthermore, the model provides the 3D geometry of the fire front, for all points: height, depth, temperature, upward gas velocity and flame tilt angle.

It must be noticed that unlike other literature models, the present model gives good results for high values of wind and slope. Changes of slope or changes of wind direction do not create a problem. If the nature of the vegetation changes, when the fire spreads, new parameters have to be identified which can be done, a priori, and saved in a database.

The validation of the model has been done with an important part of literature results for fires at laboratory scale, and also for a set of fires at field-scale. In all cases, it provides very good results. The model requires the identification of four parameters: A, b_w, b_s and c_l.

- At the beginning, we had an unknown parameter q, but it appears that the value $q = 3$ suits for all cases.
- c_l is the low rate of spread to determine for each vegetation. c_l depends on optical depth, moisture content and the volume mass.
- The parameter A depends mainly on the fuel moisture content.
- The parameters b_s and b_w depend mainly on the fuel surface mass.

With more experimental data, we wish to define relations providing those four parameters from four universal parameters (as c_{10}, A_{00}), and measurable data of the vegetation: moisture content, surface mass, optical depth, height.

The computational time is very short, because we solve algebraic equations: no mesh for the study domain is required. From the position of the fire front at the time t, we build the following one at the time $t + \Delta t$, moving each point of the fire front along the normal for a translatory motion of $c_h \cdot \Delta t$.

In a future work, we will present a detailed analysis of fire fronts shape prediction (flame height, length, tilt angle...) at laboratory and field scale, which establishes the relevance of this model. The latter should be the heart of a real-time fire-spread simulator.

NOMENCLATURE

c	rate of spread (m/s)
c_{pg}	specific heat of gas mixture (J/kg/K)
c_{pfu}	specific heat of vegetative fuel (J/kg/K)
d	depth of fuel bed (m)
D	width of the flame base (m)
g	acceleration due to gravity (m/s^2)
H	flame height (m)
h	height of the flame base (m)
l	width of the flame body (m)
$\vec{n}$	unit vector, normal of fire front
Q	heat release rate per unit length (kW/m)
R	radiant heat flux (kW/m^2)
r	distance for view factor (m)
T	temperature (K)
t	time (s)
u,v	gas velocity (m/s)
x	coordinate in space (m)
Δh_{fu}	heat of combustion of fuel (kJ/kg)
Δh_w	heat of latent evaporation (kJ/kg)

Greek

α_0	global slope angle
α	slope angle
α_{fu}	volume fraction of fuel
β	flame deviation due to wind or in draft
χ	law for fraction radiation
δ	mean penetration distance (m)
$\varepsilon\phi\lambda$	flame emissivity
γ	flame tilt angle
η	moisture content

θ	angle to calculate radiant heat flux
ρ	gas density (kg/m^3)
σ	Stefan-Boltzmann constant ($W/m^2/K^4$)
$\sigma\phi\upsilon$	surface mass of fuel (kg/m^2)
$\sigma\omega$	surface mass of water in fuel (kg/m^2)
φ	angle for calculation of view factor
τ	flame residence time
υ	stœchiometric ratio
$\xi\phi\upsilon$	surface to volume ratio of fuel (m^{-1})
Ψ	angle to calculate radiant heat flux

Subscripts

a	ambient
b	flame base
fl	flame
fu	fuel
g	gas
h	high regime
ig	ignition
l	low regime
s	slope
u	upward or upwind
w	wind

APPENDIX

Determination of β_s under Slope Condition

For the determination of β_s, we first substitute Eqs. (9) and (10) in Eq. (3). This leads to

$$\tan\beta_s = \frac{v_s}{u_{fl}} = \frac{\upsilon}{\upsilon+1}\frac{l}{h}\frac{\rho_g}{\rho_a} \approx \frac{l}{h}\frac{\rho_g}{\rho_a}$$

Then, by using Eq. (7) for the gas flowing from the flame base to the flame body, we have

$$h = \frac{l}{D}\frac{T_a}{T}H$$

By substituting this last result in the previous relationship, we obtain

$$\tan\beta_s = \frac{D}{H}$$

Finally, by using Eq. (6) and since the width of the flame base can be obtained by

$$D = c_h \tau$$

where τ is the flame residence time, which is a property of the fuel, we obtain

$$\begin{aligned} \tan\beta_s &= \frac{\tau c_h^{3/5}}{0.08(\Delta h_{fu}\sigma_{fu})^{2/5}} = b_s c_h^{3/5} \\ \text{with } b_s &= \frac{\tau}{0.08(\Delta h_{fu}\sigma_{fu})^{2/5}} \end{aligned} \tag{22}$$

Determination of β_w under Wind Condition

For the determination of β_w, we first substitute Eq. (8) in Eq. (1)

$$\begin{aligned} \tan\beta_w &= \frac{v_w}{u_{fl}} = \frac{v_w}{0.2\sqrt{\left(\frac{T_{fl}}{T_a}-1\right)gQ^{1/5}}} = \frac{v_w c_h^{-1/5}}{0.2\sqrt{\left(\frac{T_{fl}}{T_a}-1\right)g}(\Delta h_{fu}\sigma_{fu})^{1/5}} \\ &= b_w v_w c_h^{-1/5} \\ \text{with } b_w &= \frac{1}{0.2\sqrt{\left(\frac{T_{fl}}{T_a}-1\right)g}(\Delta h_{fu}\sigma_{fu})^{1/5}} \end{aligned} \tag{23}$$

REFERENCES

Albini, F.A. (1985) A model for fire spread in wildland fuels by radiation. *Combust. Sci. Technol.*, **42**, 229–258.

Anderson, H.E. and Rothermel, R.C. (1965) Influence of moisture and wind upon the characteristics of free-burning fires, Tenth Symposium (International) on Combustion, The Combustion Institute, Pittsburgh, PA, 1009–1019.

Catchpole, W.R., Catchpole, E.A., Butler, B.W., Rothermel, R.C., Morris, G.A., and Latham, D.J. (1998) Rate of spread of free-burning fires in woody fuels in a wind tunnel. *Combust. Sci. Technol.*, **131**, 1–37.

Cheney, N.P., Gould, J.S., and Catchpole, W.R. (1993) *Int. J. Wildland Fire*, **3**(1), 31–44.

Dupuy, J.L. (1995) Slope and fuel load effects on fire behaviour: laboratory experiments in pine needles fuel beds. *Int. J. Wildland Fire*, **5**(3), 153–164.

Finney, M.A. (1998) FARSITE: Fire area simulator–model development and evaluation. *USDA Forest Service Research Paper RMRS-RP-4*, Rocky Mountains Research Station, Ogden, Utah.

Grishin, A.M. (1997) Mathematical Modeling of Forest Fires and New Methods of Fighting them. Publishing house of the Tomsk state university, Albini.

Guijarro, M., Hernando, C., de Los Santos, J.A., and Diez, C. (1997) Forest FIRE behavior on the wind túnel, Hefaistos Project Report, ENV4-CT96-0299.

Larini, M., Giroux, F., Porterie, B., and Loraud, J.C. (1997) A multiphase formulation for fire propagation in heterogeneous combustible media. *Int. J. Heat Mass Trans.*, **41**(6–7), 881–897.

Markstein, G.H. (1977) Scaling of radiative characteristics of turbulent diffusion flames. *16th Interntional Symposium on Combustion*, The Combustion Institute, Pittsburgh, 1407–1419.

Martins Fernandes, P.A. (2001) Fire spread prediction in shrub fuels in Portugal. *Forest Ecol. Mgmt.*, **144**, 67–74.

McArthur, A.G. (1966) Weather and grassland fire behaviour. *Australian Forest and Timber Bureau Leaflet No. 100*.

McCaffrey, B.J. (1979) Purely buoyant diffusion flame: some experimental results, *NBSIR* 79–1910.

Mendes-Lopes, J.M., Ventura, J.M., and Amaral, J.M. (1998) *Third Int. Confer. on Fire Research, Luso*, Vol I. 497–511.

Mendes-Lopes, J.M., Ventura, J.M., and Amaral, J.M. (2003) Flame characteristics, temperature-time curves and rate of spread in fires propagating in a bed of *Pinus Pinaster* needles. *Int. J. Wildland Fire*, **12**, 67–73.

Morandini, F., Santoni, P.A., and Balbi, J.H. (2001) The contribution of radiant heat transfer to laboratory-scale fire spread under the influences of wind and slope. *Fire Safety J.*, **36**, 519–543.

Morandini, F., Simeoni, A., Santoni, P.A., and Balbi, J.H. (2005) A model for the spread of fire across a fuel bed incorporating the effects of wind and slope. *Combust. Sci. Tech.*, **177**, 1381–1418.

Morvan, D. and Dupuy, J.L. (2004) Modeling the propagation of a wildfire through a mediterranean shrub using a multiphase formulation. *Combust. Flame*, **138**, 199–210.

Porterie, B., Morvan, D., Loraud, J.C., and Larini, M. (2000) Physics of fluids, **12**(7), 1762–1782.

Pastor, E., Zárate, L., Planas, E., and Arnaldos, J. (2003) Mathematical models and calculation systems for the study of wildland fire behaviour. *Prog. Energy Combust. Sci.*, **29**, 139–153.

Rothermel, R.C. (1972) A mathematical model for predicting fire spread in wildland fuels. *United States Department of Agriculture, Forest Service*, Research Paper INT-115, International Forest and Range Experiment Station, Ogden, UT, USA, 40 pp.

Sun, L., Zhou, X., Mahalingam, S., and Weise, D.R. (2003) Experimental study on fire behaviour of live chaparral fuels. *2nd International Wildland Fire Ecology and Fire Management Congress*, P5.5

Viegas, D.X. (2004) On the existence of a steady state regime for slope and wind driven fires. *Inter. J. Wildland Fire*, **13**, 101–117.

Weber, R.O. (1989) Analytical models for fire spread due to radiation. *Combust. Flame*, **78**, 398–408.

Weber, R.O. (1990) Modelling fire spread through fuel beds. *Prog. Energy Combust. Sci.*, **17**, 67–82.

Wolfram, S. (2003) The Mathematica Book, 5th ed., Wolfram Media.